The FASEB Journal article fj.12-213462. Published online February 1, 2013.

Genetic control of estrogen-regulated transcriptional and cellular responses in mouse uterus

Emma H. Wall,* Sylvia C. Hewitt,† Liwen Liu,‡ Roxana del Rio,* Laure K. Case,* Chin-Yo Lin,§ Kenneth S. Korach,† and Cory Teuscher*,§,1

*Department of Medicine, University of Vermont, Burlington, Vermont, USA; †Receptor Biology Group and ‡Biostatistics Branch, National Institute of Environmental Health Science, National Institutes of Health, Research Triangle Park, North Carolina, USA; and §Center for Nuclear Receptors and Cell Signaling, University of Houston, Houston, Texas, USA

ABSTRACT **The uterotropic response of the uterus to 17β-estradiol (E_2) is genetically controlled, with marked variation observed depending on the mouse strain studied. Previous genetic studies from our laboratory using inbred mice that are high [C57BL/6J (B6)] or low [C3H/HeJ (C3H)] responders to E_2 led to the identification of quantitative trait QT loci associated with phenotypic variation in uterine growth and leukocyte infiltration. The mechanisms underlying differential responsiveness to E_2, and the genes involved, are unknown. Therefore, we used a microarray approach to show association of distinct E_2-regulated transcriptional signatures with genetically controlled high and low responses to E_2 and their segregation in (C57BL/6J×C3H/HeJ) F_1 hybrids. Among the 6664 E_2-regulated transcripts, analysis of cellular functions of those that were strain specific indicated C3H-selective enrichment of apoptosis, consistent with a 7-fold increase in the apoptosis indicator CASP3, and a 2.4-fold decrease in the apoptosis inhibitor *Naip1* (*Birc1a*) in C3H *vs.* B6 following treatment with E_2. In addition, several differentially expressed transcripts reside within our previously identified QT loci, including the ERα-tethering factor *Runx1*, demonstrated to enhance E_2-mediated transcript regulation. The level of RUNX1 in uterine epithelial cells was shown to be 3.5-fold greater in B6 compared to C3H. Our novel insights into the mechanisms underlying the genetic control of tissue sensitivity to estrogen have great potential to advance understanding of individualized effects in physiological and disease states.—Wall, E. H., Hewitt, S. C., Liu, L., del Rio, R., Case, L. K., Lin, C.-Y., Korach, K. S., Teuscher, C. Genetic control of estrogen-regulated transcriptional and cellular responses in mouse uterus. *FASEB J.* 27, 000–000 (2013). www.fasebj.org**

Key Words: microarray · uterotropic response · phenotypic variation · inheritance · microarray

ESTROGENS ARE FEMALE SEX hormones that are involved in a variety of physiological processes, including the development and function of reproductive tissues, wound healing, and bone growth (1, 2). Although the biological actions of estrogens are quite diverse, they are mainly known for the ability of 17β-estradiol (E_2), the primary estrogen secreted by the follicle of the ovary, to induce growth and differentiation of reproductive tissues. The physiological response of the uterus to E_2, which has been well characterized, consists of early- and late-phase responses. The early rapid phase, which occurs within 6 h of E_2 stimulation, is characterized by changes in gene transcription, a marked increase in vascular permeability, and water imbibition (3, 4). The late-phase response, which occurs 18 to 30 h after E_2 stimulus, is characterized by an influx of leukocytes into the uterine stroma, changes in transcription of late-phase genes, and an increase in epithelial cell proliferation and differentiation (4, 5). In addition, each phase of the uterotropic response is associated with distinct transcriptional signatures, implicating unique sets of differentially expressed genes in each of the physiological effects of E_2 (6).

Many physiological traits, including uterotropic responses (7–10), are continuous or quantitative in nature rather than discrete. Such traits exhibit polygenic inheritance, being controlled by quantitative trait (QT) loci, which are stretches of DNA containing or linked to the genes that underlie a quantitative trait (11). Early studies demonstrated that the uterotropic response to E_2 is genetically controlled, with marked variation in tissue growth and/or regression observed depending on the strain of mouse studied (7–10). More recently, research from our laboratory showed that the infiltration of leukocytes, particularly eosinophils, into the uterine stroma is also genetically determined (12). Our subsequent work using inbred strains of mice that are high responders [C57BL/6J (B6)] or low responders [C3H/HeJ (C3H)] to E_2 has led to the identification of

Abbreviations: B6, C57BL/6J; B6C3, (B6×C3H) F_1; B10, C57BL/10J; C3H, C3H/HeJ; CC3, cleaved caspase-3; D1, DBA/1J; D2, DBA/2J; E_2, 17β-estradiol; EdU, 5-ethynyl-2′-deoxyuridine; ERE, estrogen-response element; ESR1, estrogen receptor-α; IPA, Ingenuity Pathway Analysis; *Naip1,* NLR family apoptosis inhibitory protein 1 (Birc1a); OVX, ovariectomized; QT, quantitative trait; *Runx1*, runt-related transcription factor 1; SJL, SJL/J; SNP, single nucleotide polymorphism; TUNEL, terminal deoxynucleotidyl transferase dUTP nick end labeling

[1] Correspondence: Immunobiology Program, C331 Given Medical Bldg., University of Vermont, Burlington, VT 05405, USA. E-mail: c.teuscher@uvm.edu

doi: 10.1096/fj.12-213462

This article includes supplemental data. Please visit *http://www.fasebj.org* to obtain this information.

QT loci controlling quantitative variation in uterine growth and eosinophil infiltration (12, 13). Specifically, E_2-induced uterine growth is determined by QT loci on chromosomes 5 (*Estq2*) and 11 (*Estq3*), whereas the number of infiltrating eosinophils is controlled by QT loci on chromosomes 4 (*Estq1*) and 10 (*Estq4*) and an interactor on chromosome 16 influencing both traits.

Although it is clear that the E_2-regulated uterotropic response is genetically controlled, the mechanisms underlying the genetic control, and the genes involved, are unknown. In addition, it is unknown whether the E_2-regulated transcriptomes in high and low responders to E_2 are distinct or are similar genes regulated at different magnitudes. Therefore, we used a microarray approach to compare the E_2-regulated transcriptional response of the uterus from B6, C3H, and (B6×C3H) F_1 (B6C3) mice and discovered that the genetically controlled high and low responses to E_2 are associated with distinct transcriptional signatures and inheritance patterns. When microarray results were combined with data from our previous genetic mapping experiments, candidate genes underlying the QT loci controlling the E_2-regulated uterotropic response were identified. The identification of the genes underlying these QT loci through positional cloning and the elucidation of their functions in the uterus, and in other reproductive tissues, will provide insight into the mechanisms underlying variations in tissue sensitivity to estrogen during various physiological and disease states.

MATERIALS AND METHODS

Animals and treatments

Mouse uterotropic bioassay

All animal studies were in accordance with the guidelines of the Animal Care and Use Committee of the University of Vermont. Genetic control of uterine responsiveness to E_2 was examined by quantifying uterine peroxidase activity using the immature and/or the adult ovariectomized (OVX) mouse uterotropic assay (14). B6, C57BL/10J (B10), C3H, DBA/1J (D1), DBA/2J (D2), and SJL/J (SJL) mice were purchased from the Jackson Laboratory (Bar Harbor, ME, USA). For the immature mouse model, 2-wk-old female mice were treated at time points 0, 24, and 48 h with either E_2 (40.0 μg/kg BW i.p.) in 0.1 ml saline containing 0.25% ethanol or ethanol/saline vehicle. At 24 h after the third treatment (72 h), mice were euthanized, and uteri were collected and homogenized at 4°C in 10 mM Tris-HCl (pH 7.4) buffer. The homogenate was then centrifuged at 30,000 *g* for 45 min at 4°C, and the pellets were resuspended in T10 C500 buffer (10 mM Tris-HCL containing 0.5 M CaCl), rehomogenized, and centrifuged at 30,000 *g* for 45 min at 4°C. The supernatant was assayed for peroxidase activity using guaiacol and H_2O_2, as described previously (5, 14–16). For the adult OVX mouse assay, 8-wk-old B6 and C3H female mice were subjected to ovariectomy, rested for 1–2 wk, and treated with E_2 (40.0 μg/kg BW i.p.) in 0.1 ml saline containing 0.25% ethanol, or ethanol/saline vehicle, as described above. At 72 h, mice were euthanized, uteri were collected, and peroxidase activity was quantified.

Transcriptional and cellular responses of mouse uterus to E_2

All animal studies were in accordance with U.S. National Institutes of Health guidelines (Institute of Laboratory Animal Resources 1996) and an animal studies protocol approved by the National Institute of Environmental Health Sciences (NIEHS) Animal Care and Use Committee. The animals were treated humanely and with regard for alleviation of suffering.

Eight-week-old female B6, C3H, and B6C3 hybrid mice were purchased from the Jackson Laboratory. Animals were subjected to ovariectomy at NIEHS, rested for 1 to 2 wk, and then subjected to treatment with either E_2 (40.0 μg/kg BW i.p.) in 0.1 ml saline containing 0.25% ethanol, or ethanol/saline vehicle. For EdU labeling, animals were injected with EdU, 2 mg/ml in saline, 2 h prior to euthanasia. Animals were euthanized and tissue was collected at 2 or 24 h after injection, or at 24 h after the last of 3 daily s.c. injections of E_2 (40.0 μg/kg BW s.c.) in 0.1 ml sesame oil, or sesame oil vehicle. Uterine tissue from 4 or 5 animals/treatment group was collected; a small portion was fixed in 10% formalin, and the remainder was snap-frozen in liquid nitrogen for subsequent RNA isolation. For histology, microarray, and PCR, samples used were from the same group of animals.

Microarray analysis

Frozen uterine tissue from 3 animals/treatment group was pulverized, then homogenized in TRIzol (Invitrogen, Carlsbad, CA, USA), and RNA was prepared according to the manufacturer's protocol. Isolated RNA was then further purified using the Qiagen (Valencia, CA, USA) RNeasy mini prep kit clean-up protocol.

Gene expression analysis on each individual sample (n=3 arrays/group) was conducted using Agilent Whole Mouse Genome 4x44 Multiplex format oligo arrays (014868; Agilent Technologies, Santa Clara, CA, USA) following the Agilent 1-color microarray-based gene expression analysis protocol. Starting with 500 ng of total RNA, Cy3-labeled cRNA was produced according to manufacturer's protocol. For each sample, 1.65 μg of Cy3-labeled cRNAs were fragmented and hybridized for 17 h in a rotating hybridization oven. Slides were washed and then scanned with an Agilent scanner. Data were obtained using the Agilent Feature Extraction 9.5 software, using the 1-color defaults for all parameters. Agilent Feature Extraction performed error modeling, adjusting for additive and multiplicative noise. The resulting data were processed using Rosetta Resolver 7.2 (Rosetta Biosoftware, Kirkland, WA, USA).

To identify differentially expressed probes, an error-weighted ANOVA using multiple-test Bonferroni correction was performed using Rosetta Resolver (http://www.rosettabio.com). Data were analyzed using a threshold of $P < 0.001$ to identify differentially expressed probes. Hierarchical clusters were constructed using Entrez genes that met the following cutoffs: $P < 0.001$ and absolute value of fold change > 2. Data sets were deposited into the Gene Expression Omnibus (GEO; GSE38800; http://www.ncbi.nlm.nih.gov/geo/).

Two similar experiments were conducted for confirmation of differential gene expression (data not shown). In the first confirmation experiment, strains, treatments, and times of tissue sampling were identical to those described above, and gene expression was assessed using Affymetrix GeneChip 430A 2.0 Mouse Genome Arrays (Affymetrix, Santa Clara, CA, USA). In the second confirmation experiment, strains and treatments were also as described above; tissues were collected at 72 h after E2 treatment, and gene expression was assessed using Illumina Mouse WG-6 v2.0 Expression Bead Chip Arrays (Illumina, San Diego, CA, USA).

Pathway analysis

Ingenuity Pathway Analysis (IPA; Ingenuity Systems, Redwood, CA, USA; http://www.ingenuity.com) was used to determine the functions enriched by genes that were unique responders to E_2 in B6 *vs.* C3H; genes, containing nonsynonymous single-nucleotide polymorphism (SNP) between B6 and C3H that reside within previously identified QT loci; and genes that were differentially expressed between B6 and C3H control animals and reside within previously identified QT loci. The Agilent Whole Mouse Genome 4x44 array was used as a reference for the analysis, and all other options used were default settings in IPA. Significance of enriched functions was adjusted for multiple hypotheses testing using the Benjamini-Hochberg method (17).

SNP analysis

To gain insight into the genes that might be involved in regulatory mechanisms influencing differential gene expression across strains in response to E_2, we conducted SNP analysis on genes located within previously identified QT loci that control the uterine response to E_2 (12, 13). Regions selected for SNP analysis were based on markers that showed significant linkage to either uterine weight or eosinophil infiltration in response to E_2 (12, 13) and included chromosome 4 (*Estq1*): 8,256,102 to 66,843,205; chromosome 5 (*Estq2*): 28,676,908 to 47,836,375; chromosome 10 (*Estq4*): 113,818,252 to 129,817,889; chromosome 11 (*Estq3*): 54,003,617 to 112,374,590; and chromosome 16: 11,616,475 to 92,807,411. Genes within each of these regions were identified and subjected to SNP analysis using the Mouse Phenome Database (http://phenome.jax.org/SNP).

Histological analyses

For histological analyses, fixed uteri were embedded in paraffin, sectioned at ~4-μm thickness, and mounted onto silanized slides.

Immunofluorescence

An anti-runt-related transcription factor 1 (RUNX1)/AML1 rabbit monoclonal antibody (Abcam, Cambridge, MA, USA) was used to determine the expression pattern of RUNX1 in the uterus. For cleaved caspase-3 (CC3), an anti-CC3(D175) rabbit polyclonal antibody (Cell Signaling, Danvers, MA, USA) was used. For estrogen receptor-α (ESR1), an anti-ESR1 mouse monoclonal antibody (PN IM1545; Beckman Coulter, Brea, CA, USA) was used. Slides were deparaffinized using a series of xylene/ethanol washes, followed by a final rinse in dH_2O. Antigen retrieval was performed using Dako Target Retrieval Solution (Dako, Carpinteria, CA, USA). Slides were incubated in retrieval solution for 20 min, allowed to cool for 10 min, and then washed twice in dH_2O. Briefly, the immunohistochemistry protocol was as follows: a 10-min incubation in PBS and 1% BSA, followed by a 15-min incubation in 1% BSA/0.1% Triton X-100 solution. Slides were then washed twice for 10 min/wash in PBS and 1% BSA. Blocking was performed by incubating slides for 30 min in 10% normal goat serum in PBS and 1% BSA. Slides were incubated overnight at room temperature with primary antibody, diluted 1:100 in PBS and 1% BSA. The following day, slides were washed twice for 5 min/wash in PBS and 1% BSA, followed by a 60-min incubation with secondary antibody (goat anti-rabbit Alexa Fluor 555; Invitrogen) diluted 1:500 in PBS and 1% BSA, followed by another 2 washes of 5 min/wash in PBS and 1% BSA. Slides were then incubated for 15 min with DAPI diluted 1:200 in PBS and 1% BSA, washed twice for 5 min in PBS and 1% BSA, and coverslips were applied using Aqua Polymount (Polysciences, Inc., Warrington, PA, USA).

The detection of 5-ethynyl-2′-deoxyuridine (EdU; Click-iT EdU imaging kit, Invitrogen) was conducted according to the manufacturer's protocol, with the amount of Alexa Fluor 488 increased to 5 μl/ml of Click-iT reaction cocktail.

Imaging

Optical sections (2 μm thick) were acquired with a Zeiss 510 META confocal microscope (Carl Zeiss MicroImaging, LLC, Thornwood, NY, USA) using a ×20 Plan Apochromat lens. Images were captured using a sequential scan in channel mode with a 1024 × 1024 frame size and 12-bit depth. Signal for RUNX1, CC3, or ESR1 was captured using a 543 helium neon laser and a long-pass LP 560 emission filter. For EdU, the signal was analyzed by using fluorescence microscope with 495-nm excitation and 519-nm emission wavelengths. Hoechst dye was used as a counterstain to visualize tissue using 350-nm excitation and 461-nm emission wavelengths.

Image analysis

Quantification of RUNX1, CC3, or ESR1 expression was performed using MetaMorph 7.7.3 64-bit offline software (Molecular Devices, Sunnyvale, CA, USA). At least 2 fields/sample were imaged and quantified, and all samples were coded to prevent observer bias. For all samples, an inclusive threshold was used with a lower limit of 1500 and an upper limit of 4095 (default maximum). The regional measurements tool was used to quantify the integrated intensity of RUNX1, CC3, or ESR1 staining in the luminal and glandular epithelium.

Immunohistochemistry

Terminal deoxynucleotidyl transferase dUTP nick-end labeling (TUNEL) staining was conducted by using the ApopTag Plus peroxidase *in situ* apoptosis kit (cat. S7101; Millipore, Bedford, MA, USA) according to the manufacturer's protocol. Ki67 was detected after decloaking with heat and pressure for 3 min in citrate buffer in a decloaking chamber (Biocare, Walnut Creek, CA, USA), blocking with 3% H_2O_2 (Fisher Scientific, Fairlawn, NJ, USA) for 10 min, followed by 5% normal rabbit serum (Santa Cruz Biotechnology, Santa Cruz, CA, USA) for 10 min. Anti-Ki67 (TEC 3; DakoCytomation, Carpinteria, CA, USA) diluted 1:80 in automation buffer (Biocare, Tempe, AZ, USA) was applied for 1 h at room temperature, followed by biotinylated rabbit anti-rat IgG (Vector Laboratories, Burlingame CA, USA) diluted 1:300 for 30 min at room temperature. Avidin-biotin peroxidase complex (Vector Laboratories) was applied for 30 min, and 3,3′-diaminobenzidine substrate (DakoCytomation) was used to develop the signal. Slides were counterstained in hematoxylin (Sigma-Aldrich, St. Louis, MO, USA), dehydrated, and coverslipped.

Real-time quantitative RT-PCR

RNA was prepared from animals treated as described for microarray samples (3–5 mice/treatment group). cDNA was prepared from individual uteri and analyzed by SYBR Green real-time PCR using methods and primers previously described in Hewitt and Korach (18). Computed values for each transcript were relative to B6 vehicle. Select genes were chosen for validation to confirm differential expression between strains at baseline (*Coro2a*, *Runx1*,

Stat5b, *Trim16*), 2 h after E_2 treatment (*Klk1b3* and *Trim15*), and/or 24 h after E_2 treatment (*Msc* and *Slc2a5*).

Primer sequences were designed using Primer Express software (Applied Biosystems, Carlsbad, CA, USA) or were copied from PrimerBank (http://pga.mgh.harvard.edu/primerbank/) and were as follows: *Coro2a* forward, GCAATGGAAGCAGTACAAAGCT, *Coro2a* reverse, GGTGTGTGCAGATACCAGCG; *Klk1b3* forward, AGAGATGGATGGAGGCAAAGAC, *Klk1b3* reverse, TGGAGAACACCATCACAGATCAG; *Msc* forward, GCCTGGCTTCCAGCTACATC, *Msc* reverse, CACGTCAGGTTCACAGGGTG; NLR family apoptosis inhibitory protein 1 (*Naip1*) forward, AGTGAGAAGGCAGCAAGCAG; *Naip1* reverse, CGCAGTCTCCTGGTTAGCAC; *Runx1* forward, GAGATTCAACGACCTCAGGTTT; *Runx1* reverse, TGTAAAGACGGTGATGGTCAGA; *Slc2a5* forward, CTCATCCTTCCAATATGGGTACAAC, *Slc2a5* reverse, AGGTGTCATTGTAAAACTGCTGCAT; *Stat5b* forward, CTGTTTGACTCACAGTTCAGCG, *Stat5b* reverse, GGGAGCGACAAGGTCTTGAC; *Trim15* forward, AACCAGCAAGTGAGCTTCTGC, *Trim15* reverse, CCTCTGGGCTCACAAAAGTCTT; *Trim16* forward, TGGAGGTGGCACCTATGTTG, *Trim16* reverse, AATGCAGCTGTTCCGTTCTTC.

Statistical analyses

Data were subjected to 2-way ANOVA using the mixed procedure of SAS 9.1 (SAS Institute, Cary, NC, USA) to determine the effect of strain, E_2 treatment, and the strain by treatment interaction on gene expression measured by quantitative PCR and on expression of CC3, ESR1, EdU, and Ki67 in uterine epithelium. The model included treatment and time as fixed variables and mouse as a random variable. The comparison of means between strains at each time point was performed using Fisher's protected LSD test, and significance was declared at $P < 0.05$. To determine the effect of parental strain on expression of RUNX1 in uterine tissue, data from B6 and C3H vehicle-treated control animals were $\log_{10}$ transformed to achieve a normal distribution and were then subjected to a 1-tailed *t* test within SAS. Significance was declared at $P < 0.05$.

RESULTS

Genetic control of the E_2-regulated uterotropic response

To determine the degree to which genotype influences uterine responsiveness to E_2, uterine peroxidase activity was used as a quantitative trait variable for assessing phenotypic variation in the immature and/or adult OVX mouse uterotropic assay (14). As expected, there was a highly significant effect of E_2 on uterine peroxidase activity across all strains ($P<0.001$; **Fig. 1*A***). In addition, among the 6 different inbred strains studied, there was a marked effect of strain as well as a treatment by strain interaction ($P<0.001$; Fig. 1*A*) with a continuous distribution of uterine peroxidase activity, indicative of polygenic inheritance (19, 20). Using this assay, we found that B6 was the highest responder to E_2, whereas C3H was the lowest. The results obtained with immature B6 and C3H mice were confirmed in adult OVX mice (Fig. 1*B* and refs. 12, 13).

Strain-specific transcriptional responses to E_2

To determine the role of genotype in controlling the transcriptional response of the uterus to E_2, we conducted a microarray experiment on uterine tissue from B6, C3H, and B6C3 mice at 2 and 24 h after treatment with E_2. The results of the microarray experiment revealed 6664 genes that were E_2 regulated in ≥1 strain during ≥1 time point ($P<0.001$ and signed fold change >2; GEO data set GSE38800). Hierarchical clustering of those genes confirmed distinct early- and late-phase transcriptional signatures associated with the physiological response to E_2 in all of the strains (**Fig. 2**). In addition, it was clear that there were strain-specific responses at each time point. To identify common genes that were regulated by E_2 in all strains, as well as those that were strain-specific, all E_2-regulated genes were subjected to correlation analysis within Resolver. **Figure 3** illustrates the results of comparing differential gene expression at 2 h in B6 *vs.* C3H, and similar results were observed across all strain comparisons at both time points (data not shown). Specifically, at each time point, there was a clear common transcriptional response, in both the identity of responsive genes and their magnitudes of change, to E_2 across the strains such that for each comparison, the correlation coefficient of common signature gene responses was ≥0.88 ($P<0.001$; Fig. 3*A*).

We also identified genes that were uniquely regulated by E_2 in each strain (Fig. 3*B*). Venn diagrams were then generated to summarize the common and distinct E_2-regulated genes in parental strains (Supplemental Fig. S1*A*), and all strains at 2 and 24 h (Supplemental Fig. S1*B*). Supplemental Fig. S1*B* also illustrates the inheritance pattern of the transcriptional response to E_2; the transcriptional responses were in some cases inherited in a mendelian fashion (B6C3 were similar to one parental strain) and in other cases were not, being indicative of epistasis. Confirmation of differential expression of several genes within QT loci (*Cora2a*, *Runx1*, *Stat5b*, *Trim16*), and some that were differen-

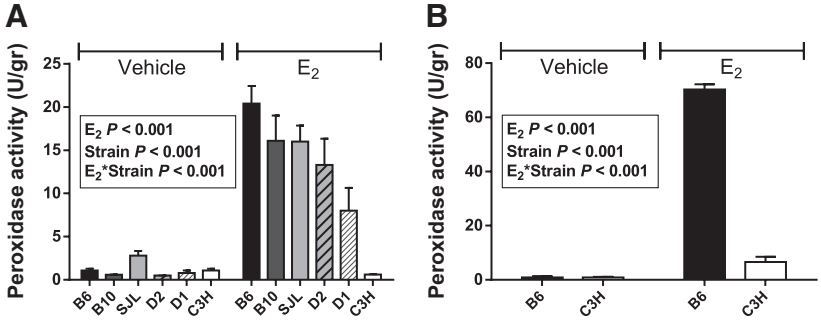

Figure 1. Uterine peroxidase activity of immature (*A*) and adult (*B*) ovariectomized inbred strains of mice (n=5–8 mice/group) at 24 h after 3 daily injections of E_2 or vehicle carrier.

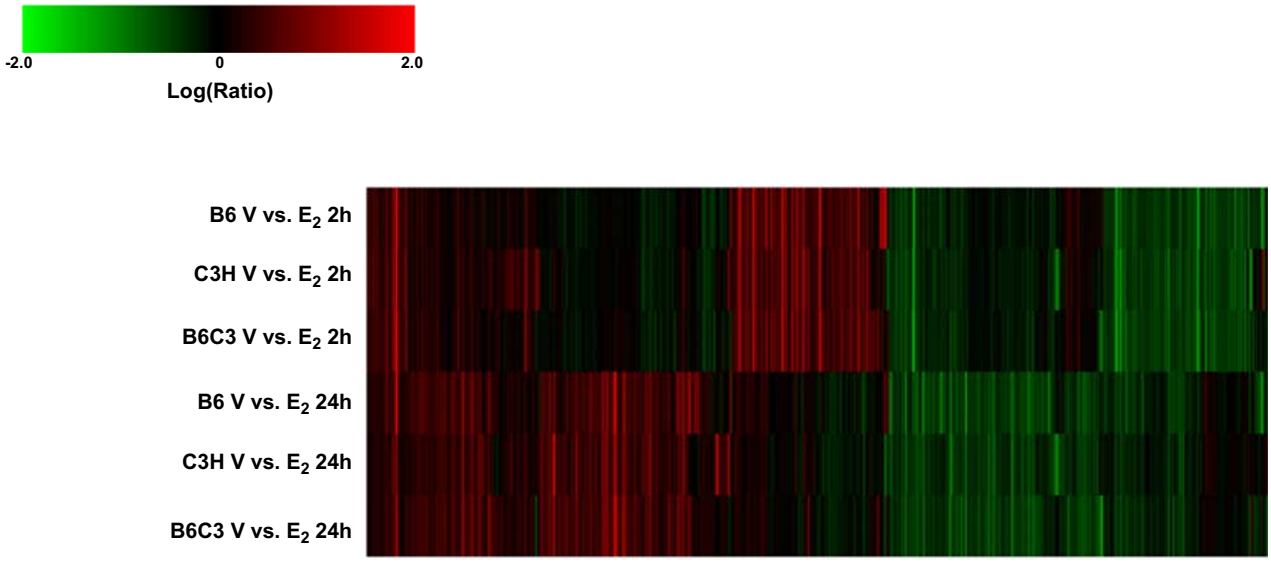

Figure 2. Hierarchical clustering reveals distinct transcriptional signatures associated with the uterine response to E_2 at 2 *vs.* 24 h. V, vehicle.

tially expressed in control animals but not located within QT loci, was performed using RT qPCR (Supplemental Fig. S2). In agreement with microarray findings, the results of RT qPCR showed differential expression between strains at baseline (*Coro2a*, *Klk1b3*, *Slc2a5*, and *Trim16*), 2 h after E_2 treatment (*Coro2a*, *Klk1b3*, *Runx1*, *Stat5b*, and *Trim15*), and/or 24 h after E_2 treatment (*Coro2a*, *Klk1b3*, and *Trim15*). For several genes, there was also a clear differential response to E_2 across strains, demonstrated by a treatment by strain interaction (*Coro2a*, *Klk1b3*, *Trim15*, *Msc*, and *Slc2a5*).

IPA was used to infer the functions associated with the distinct transcriptional responses of B6 and C3H mice to E_2 at each time point (strain-specific genes shown in Supplemental Fig. S1*A*; IPA results not shown). At 2 h after E_2 treatment, there were many functions enriched within the uterine transcriptomes of C3H mice. In contrast, the E_2-regulated uterine transcriptomes of B6 mice were associated with the enrichment of only 6 cellular functions. Treatment of C3H mice with E_2 was associated with enrichment of acute-phase signaling at 2 h, whereas no canonical pathways were significantly enriched by E_2 treatment in B6 mice. Similar results were observed at 24 h: the E_2-regulated uterine transcriptome of C3H mice was associated with enrichment of many functions and some canonical pathways, and there was very little overlap in functions enriched across the two strains. In addition, cell death pathways were significantly enhanced in C3H but not B6 mice at 2 and 24 h after treatment with E_2, and IPA predicted an increase in apoptosis in C3H at 24 h (Z score 2.1; $P<0.01$).

Identification of candidate genes for QT loci controlling the uterine response to E_2

Polymorphism in either regulatory regions controlling transcriptional activity or protein structure can serve as

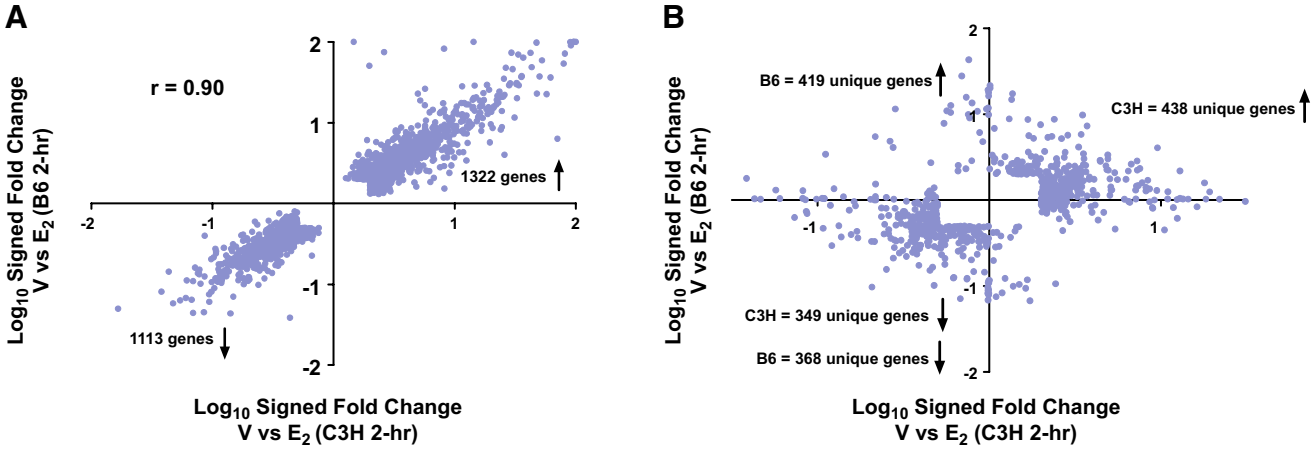

Figure 3. Comparison of the transcriptional response of the uterus to E_2 in B6 and C3H mice. Correlation analysis was conducted in Rosetta Resolver and included genes with a signal intensity of ≥100 in ≥1 sample, and ≥2-fold change in expression in ≥1 treatment condition. *A*) Common transcripts responsive to E_2 in B6 and C3H mice at 2 h post-treatment. *B*) Unique transcripts responsive to E_2 in one strain and not the other at 2 h posttreatment. Similar results were observed for 24 h. V, vehicle.

candidates for QT loci underlying the uterine response to E_2. Genes that were differentially expressed between B6 and C3H control animals, representing basal gene expression differences between strains, were hypothesized to be candidate genes based on expression level polymorphism. There were >1600 genes differentially expressed between B6 and C3H at baseline (GEO data set GSE38800), and 84 of those genes reside within the QT loci controlling the E_2-regulated uterotropic response (**Fig. 4**). The results of IPA indicated that differential expression of these genes between control animals was associated with several functions, including decreased cellular differentiation, increased cell proliferation, and increased tissue development in B6 mice (data not shown). In addition, differential expression of *Runx1* was implicated in most of the significantly enriched functions.

An additional SNP-based approach designed to identify polymorphisms within the protein coding region of genes located within the QT loci (12, 13) revealed the existence of more than 224,000 SNP between B6 and C3H mice. To identify polymorphisms in genes that may influence protein structure and/or function, we filtered this data set to include only nonsynonymous SNPs that resulted in an amino acid changes or influenced splicing (**Fig 5**). On the basis of IPA findings, the candidate genes containing nonsynonymous SNPs between B6 and C3H were predicted to influence several cellular functions related to the uterotropic response, including tissue development and tissue morphology (data not shown). In addition, many of these polymorphic genes were also differentially expressed at the transcriptional level between B6 and C3H control animals (Fig. 4).

Uterine epithelial cell apoptosis is increased after treatment with E_2 and is genetically regulated

Because pathway analysis suggested initiation of uterine cellular apoptosis selectively in C3H after treatment with E_2, we measured TUNEL-positive epithelial cells (**Fig. 6*A***), as well as expression of the apoptosis marker CC3 in uterine sections 72 h after E_2 treatment (Fig. 6*B*). TUNEL-positive epithelial cells, as well as those expressing CC3, were nearly undetectable in B6 mice, whereas they were readily visible in the uterine epithelium of C3H and B6C3 mice (Fig. 6*A*, *B*). Quantification of cellular staining confirmed these visual observations, with CC3 expression higher in both C3H and B6C3 relative to B6 ($P<0.01$; Fig. 6*C*), indicating the uterine epithelia of these strains is undergoing apoptosis. We then measured mRNA expression of the apoptosis inhibitor *Naip1* (*Birc1a*) and found that, consistent with increased apoptosis in C3H and B6C3 mice, expression of *Naip1* was decreased in those mice relative to B6 ($P<0.001$; Fig. 6*D*).

Uterine epithelial cell proliferation is increased after treatment with E_2 and is genetically regulated

Because E_2 is known to elicit cellular proliferation in uterine epithelium, we quantified the level of uterine epithelial cells labeled with EdU (**Fig. 7*A***) and Ki67 (Fig. 7*B*). Although the number of proliferating cells was

Chromosome 4	B6 vs C3H
4930412C18Rik	-6.3
Rragd	-2.8
Coro2a	5.1
2610301B20Rik	2.5
1700003M02Rik	-6.7
Gm136	-2.1
Ccl27a	2.8
Fancg	12.8
Exosc3	-3
Ube2j1	3.8
2310028H24Rik	2.1
5430416O09Rik	-2.2
AI314180	-6
Alad	-3.2
Col27a1	32

Chromosome 5	B6 vs C3H
Fosl2	-11.3
Whsc1	2.2
Nat8l	-3.4
D5Ertd579e	2.2
A930005I04Rik	5.5
Jakmip1	3.5
Lcorl	-2.3
Abhd1	-2.8
Depdc5	-7.5

Chromosome 10	B6 vs C3H
Ppm1h	-6.2
Agap2	-2.2
Cpm	2.1
Slc26a10	-7.8
Rnf41	4.5

Chromosome 11	B6 vs C3H
Lyrm7	-2.1
Sparc	-2.3
Zfp672	2.3
2210407C18Rik	-9.5
Slc6a4	-3.5
Rad51l3	2.1
Slfn8	15
Gm11428	3.9
Mpo	-2.6
Cuedc1	-6.7
Gngt2	4.2
Krt23	5.3
Cd300lg	4.2
Lsm12	5
Slc16a6	-9.2
Gpx3	2.4
Anxa6	3.1
Lrrc48	-2.7
Top3a	2.3

Chromosome 11	B6 vs C3H
Trim16	60
Trpv3	5.2
Ppm1d	3.2
Tubd1	2.4
Samd14	2.3
Krt20	8.5
Fzd2	5.7
Mapt	2.3
Mrc2	3.2
Hist3h2ba	3.1
Obscn	2.9
Pemt	-100
Myh8	-2.1
Gosr1	-2.6
Ngfr	3.2
1110035M17Rik	-2.6
Copz2	3.8
Stat5b	2
Sost	-17.3
Mpp3	-3.7
Itgb3	9

Chromosome 16	B6 vs C3H
Mkl2	-2.1
2900011O08Rik	7.1
Adipoq	4.2

Chromosome 16	B6 vs C3H
Mfi2	-2.6
Retnla	3.3
Gart	-2.1
Pdxdc1	7.4
Sema5b	-2.2
Slc15a2	14
Morc1	-2.6
Slc35a5	4.5
Atg3	2.2
Mrap	-3
Clic6	-3.6
Runx1	**5.2**

Figure 4. Genes that are differentially expressed between B6 and C3H control mice and that reside within QT loci controlling the uterine response to E_2. Numbers indicate fold change in uterine gene expression ($P<0.001$ and signed fold change ≥2; genes with positive numbers were greater in B6). Color coding indicates inheritance pattern for each gene: red, B6 inheritance; blue, C3H inheritance; green, nonmendelian inheritance (gene expression in offspring was distinct from parental strains).

Chromosome 4	Chromosome 4	Chromosome 5	Chromosome 10	Chromosome 11	Chromosome 11
Ints8	*Anks6*	*Cpz*	*Hsd17b6*	*Larp1*	*Butr1*
1110037F02Rik	*Smc2*	*Ccdc96*	*Timeless*	*Gemin5*	***Obscn***
Rad54b	*Slc44a1*	***D5Ertd579e***	*Apon*	*Mrpl22*	*Mrpl55*
Cpne3	*Zfp462*	*Gm1043*	*Stat2*	*Igtp*	*Prss38*
Fam82b	*Rad23b*	*Evc*	*Pan2*	*Irgm2*	*Zfp867*
Ggh	*Ikbkap*	*Evc2*	*Erbb3*	*Zfp692*	*Zkscan17*
Mdn1	D730040F13Rik	*Stk32b*	*Dgka*	*Gm9900*	*Olfr223*
Gabrr2	*Epb4.1l4b*	*Otop1*	*Olfr9*	2210415F13Rik	*Olfr225*
Pm20d2	*Olfr267*	*Clnk*	*Olfr765*	1810065E05Rik	*Mprip*
Orc3	*Zkscan16*	4930431F12Rik	*Olfr768*	*Gm12253*	*Srebf1*
Slc35a1	*Ptgr1*	*Lap3*	*Olfr771*	*Olfr332*	***Lrrc48***
Zfp292	AI481877	*Ncapg*	*Olfr775*	*Olfr331*	*Myo15*
Ubap2	*Susd1*	**Chromosome 10**	*Olfr782*	*Olfr328*	*Flii*
Kif24	*Slc46a2*	*Nup107*	*Olfr788*	*Olfr224*	*Smcr7*
Pigo	*Mup5*	*Mdm1*	*Olfr790*	*Olfr325*	*Smcr8*
B230312A22Rik	*Mup3*	*Mon2*	*Olfr796*	*Olfr324*	*Zfp286*
Gba2	*Mup21*	*Avil*	*Olfr799*	2210407C18Rik	***Trim16***
Spag8	*Zfp37*	*Fam119b*	*Neurod4*	*Olfr323*	*Fam18b*
4930412F15Rik	***Col27a1***	*Mettl1*	**Chromosome 11**	*Trim58*	*Myh1*
Olfr70	**Chromosome 5**	***Agap2***	*Nipsnap3b*	*Olfr179*	***Myh8***
Hrct1	*Rbm33*	*Os9*	*Csf2*	*Olfr320*	*Glp2r*
Olfr155	*Cgref1*	***Slc26a10***	*Il3*	*Olfr319*	*Rnf222*
Melk	*Cad*	*Arhgef25*	4930404A10Rik	*Olfr317*	*Aurkb*
Frmpd1	*Gm9924*	*Mbd6*	***Anxa6***	*Olfr316*	*Hes7*
Rg9mtd3	*Gm10463*	*Gli1*	*Fat2*	*Olfr313*	*Aloxe3*
1300002K09Rik	C330019G07Rik	*Inhbc*	*Fam114a2*	*Olfr311*	*Chd3*
E230008N13Rik	*Depdc5*	*Shmt2*	*Mfap3*	*Gm12258*	*Cyb5d1*
Tstd2	*Poln*	*Nxph4*	*Galnt10*	2810021J22Rik	*Tmem102*
Tbc1d2	*Nop14*	*Zbtb39*	*Gm11003*	*Zfp39*	*Nlgn2*

Chromosome 11	Chromosome 11	Chromosome 11	Chromosome 11	Chromosome 16
Kif1c	*Olfr794*	*Epn3*	2300003K06Rik	*Shisa9*
Nlrp1a	*Lpo*	*Mycbpap*	*Gast*	*Mkl2*
Nlrp1b	*Mks1*	*Rsad1*	*Klhl11*	*Parn*
Itgae	*Epx*	*Acsf2*	*Zfp385c*	***Pdxdc1***
Trpv1	*Olfr462*	*Eme1*	*Naglu*	A630010A05Rik
Trpv3	*Olfr463*	*Gm11541*	*Tubg1*	*Pi4ka*
Aspa	*Olfr464*	*Sgca*	*Ramp2*	*Vwa5b2*
E130309D14Rik	*Vezf1*	***Samd14***	*Cntd1*	*Uts2d*
Hic1	***Cuedc1***	*Itga3*	*G6pc*	***Mfi2***
Rtn4rl1	*Akap1*	*Gm9796*	*Aarsd1*	*Bex6*
Rnmtl1	*Scpep1*	*Gip*	*Rundc1*	*Tm4sf19*
Timm22	*Gm15698*	*Ube2z*	*Brca1*	*Zdhhc19*
Slc6a4	*Coil*	*Atp5g1*	***Sost***	*Tnk2*
Ccdc55	*Trim25*	*Cdk12*	***Mpp3***	*Muc4*
Fam58b	*Dgke*	*Erbb2*	*Asb16*	1700021K19Rik
Gm9964	4932411E22Rik	*Ikzf3*	*Tmub2*	
Unc45b	*Ankfn1*	*Casc3*	*Fam171a2*	
Slfn5	*Pctp*	*Tns4*	*Itga2b*	
Slfn9	*Tmem100*	*Krt28*	***Fzd2***	
Slfn8	*Stxbp4*	*Krt10*	*Lrrc37a*	
Slfn2	*Cox11*	*Krt12*	*Gm884*	
Pex12	*Tom1l1*	***Krt20***	*Myl4*	
1700020L24Rik	*Utp18*	*Krt39*	*Mrc2*	
Expi	*Spag9*	*Krt40*	*Scn4a*	
Synrg	*Tob1*	*Gm11939*	*Polg2*	
Dusp14	*Wfikkn2*	*Krtap1-3*	*Bptf*	
Prr11	*Abcc3*	*Krtap9-3*	*Ccdc46*	
Bzrap1	*Cacna1g*	*Krtap4-1*	9930022D16Rik	
Mpo	*Spata20*	*Krtap4-2*		

Figure 5. Genes that are polymorphic between B6 and C3H mice and that reside within QT loci controlling the uterine response to E_2. Genes in bold were differentially expressed between B6 and C3H mice ($P<0.001$ and signed fold change ≥ 2).

low in vehicle-treated controls, there were clear differences across the strains. Specifically, the number of EdU-positive cells was greater in C3H animals than B6 or B6C3 ($P<0.01$; Fig. 7*A*), and the number of Ki67-positive cells was greater in C3H and B6C3 than B6 ($P<0.01$; Fig. 7*B*). Across all strains, treatment with E_2 markedly induced the number of positive cells for both proliferation markers (Fig. 7*A*, *B*). Notably, uterine epithelial cell expression of ESR1, which is dispensable for eliciting an E_2-regulated uterine proliferative responsiveness but critical for inhibition of apoptosis (21), was not different across the strains ($P>0.70$; **Fig. 8*A*, *B***).

Identification of *Runx1* as a candidate for an epistatic interactor in E_2-regulated responses

Runx1 resides within a QT locus on chromosome 16 that was previously shown to exhibit epistatic interactions across E_2-regulated uterine phenotypes (12, 13) and was also differentially expressed in B6 *vs.* C3H in vehicle-treated control animals (Fig. 4). In addition, it has been suggested that some E_2-regulated changes in gene expression are the result of interactions between RUNX1 and ESR1 (22), and *Runx1* was associated with many of the functions

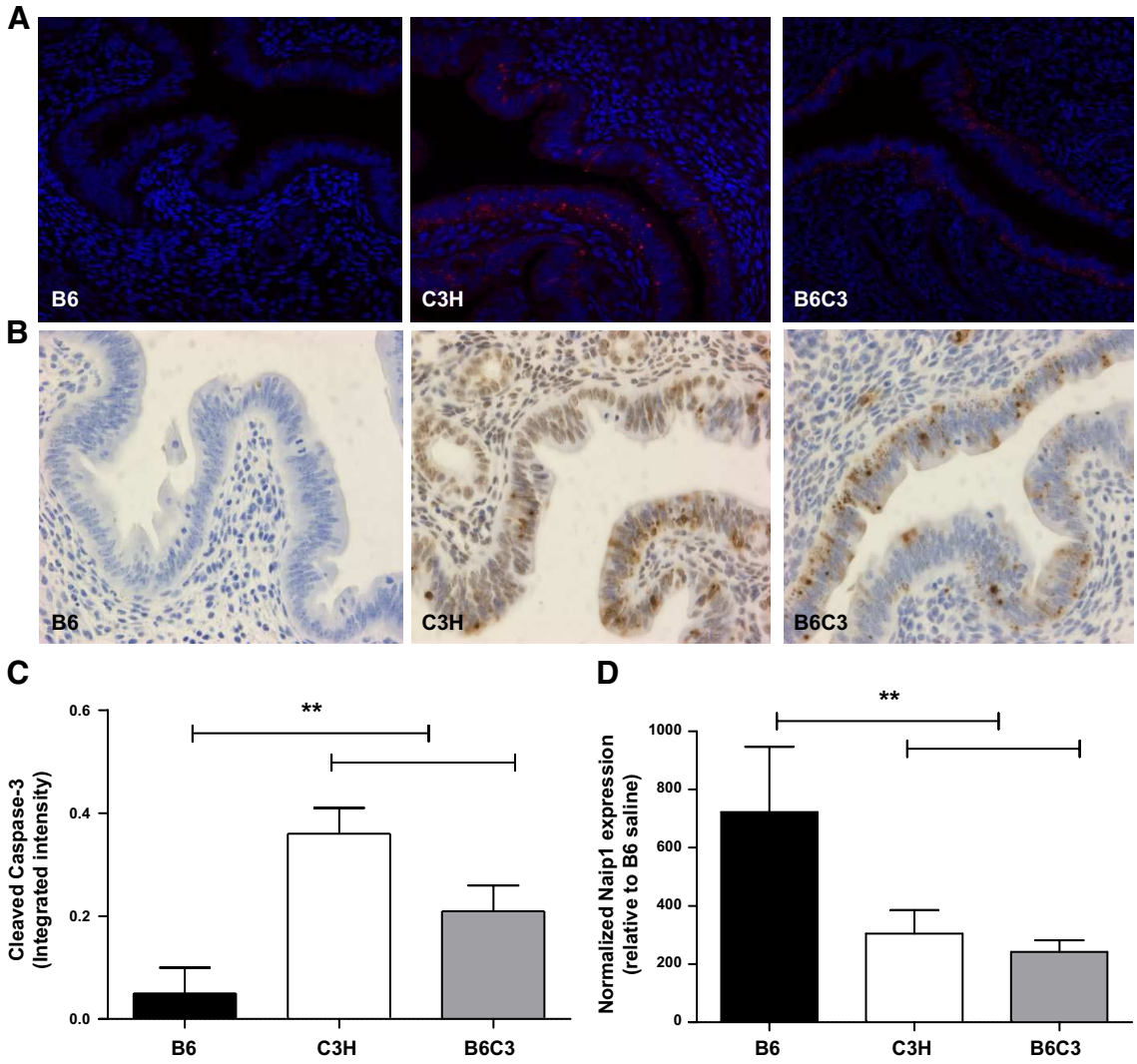

Figure 6. Apoptosis in uterine epithelium 72 h after treatment with E_2. *A*) Localization of CC3 (red, CC3; blue, DAPI; ×20 view). *B*) Localization of TUNEL-positive cells (brown, TUNEL-positive; blue, hematoxylin). *C*) Quantity of CC3 expression in uterine epithelium of B6, C3H, and B6C3 mice. *D*) Uterine expression of *Naip1* mRNA.

enriched by genes differentially expressed in control animals (data not shown). Therefore, we conducted experiments to localize and quantify the expression of RUNX1 in the uterus (**Fig. 9*A***). Cells expressing RUNX1 were mainly restricted to luminal and glandular epithelia, as well as immune cells that appeared to be infiltrating the uterine stroma. Quantification of the RUNX1 signal showed significantly more RUNX1 in B6 epithelial cells compared to C3H ($P<0.02$; Fig. 9*B*). In all strains, however, there was a marked increase in RUNX1 expression 24 h after treatment with E_2 ($P<0.001$; Fig. 9*B*).

DISCUSSION

The transcriptional response to E_2 mirrors the biphasic physiological response

In agreement with previous reports (21, 23), we observed distinct transcriptional signatures associated with the biphasic uterine response to E_2. Although the magnitude of the growth response is genetically controlled, the uterine tissue of all three strains undergoes a classical biphasic uterotropic response to E_2, including an increase in uterine weight resulting from hyperemia and hyperplasia, as well as infiltration of leukocytes (12, 13). Thus, it is not surprising that most of the transcriptional responses associated with these physiological processes were similar across strains. Our findings are more supportive of a role for genetics in the hyperplasia, as we see no strain difference in regulation of *Aqp5* or *Muc1* (data not shown); AQP5 is a water channel implicated in E_2-regulated water imbibition (24). Perhaps the E_2-regulated transcripts that were common to all three strains are those involved in the immediate-early murine uterine genomic response that occurs within <2 h of E_2 treatment. Indeed, many of the common E_2-regulated transcripts have been previously associated with the classical E_2-regulated uterotropic response in the mouse (23).

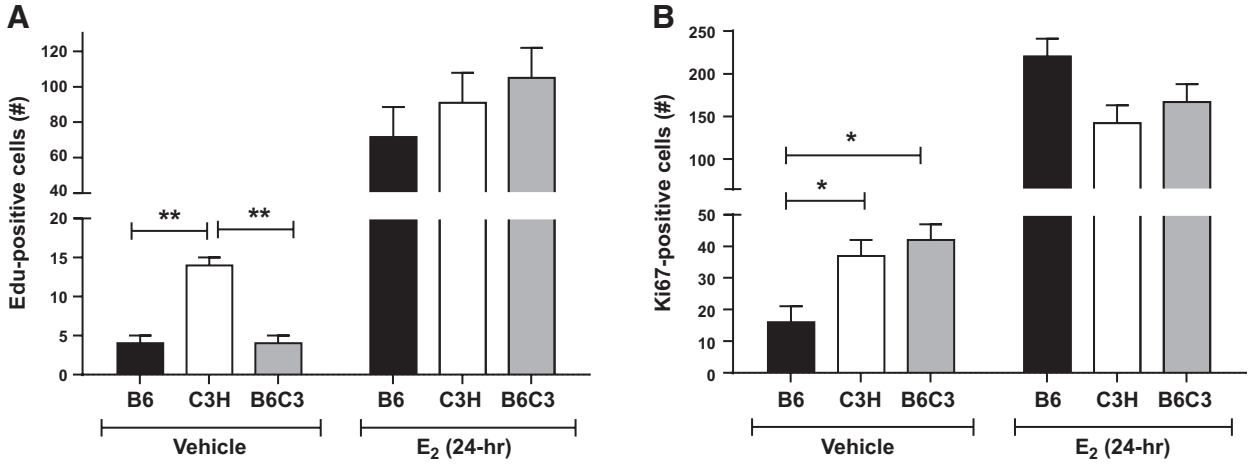

Figure 7. Proliferation in uterine epithelium at baseline and 24 h after treatment with E_2. *A*) Number of EdU-positive cells in uterine epithelium of B6, C3H, and B6C3 mice. *B*) Number of Ki67-67 positive cells in uterine epithelium of B6, C3H, and B6C3 mice.

Strain-specific responses to E_2

In addition to the genetic control of the uterotropic response, quantitative variation in the responsiveness of a variety of tissues to E_2, including bone, mammary gland, and uterus, has been observed (7, 10, 25–28). Furthermore, on the basis of our analysis of different inbred strains of mice included in the Mouse Phenome Database, many E_2-regulated phenotypes were significantly different between B6 and C3H, including fecundity index, oocytes produced per donor during superovulation, body mass index, femur thickness, and bone mineral density ($P<0.001$; data not shown). Moreover, many E_2-regulated responses exhibit significant quantitative variation in humans (29, 30). Therefore, understanding the genetic control of uterine responsiveness to E_2 has clear functional implications. In the current experiment, the increase in uterine weight 72 h after E_2 treatment was greater in B6 mice compared to C3H ($P<0.001$; data not shown), which is consistent with previous observations (12, 13). Therefore, the strain-specific transcriptional signatures that we observed at both time points may include genes that are involved in the regulation of the magnitude of the physiological response to E_2. Included among the strain-specific cellular functions were tissue and cellular development,

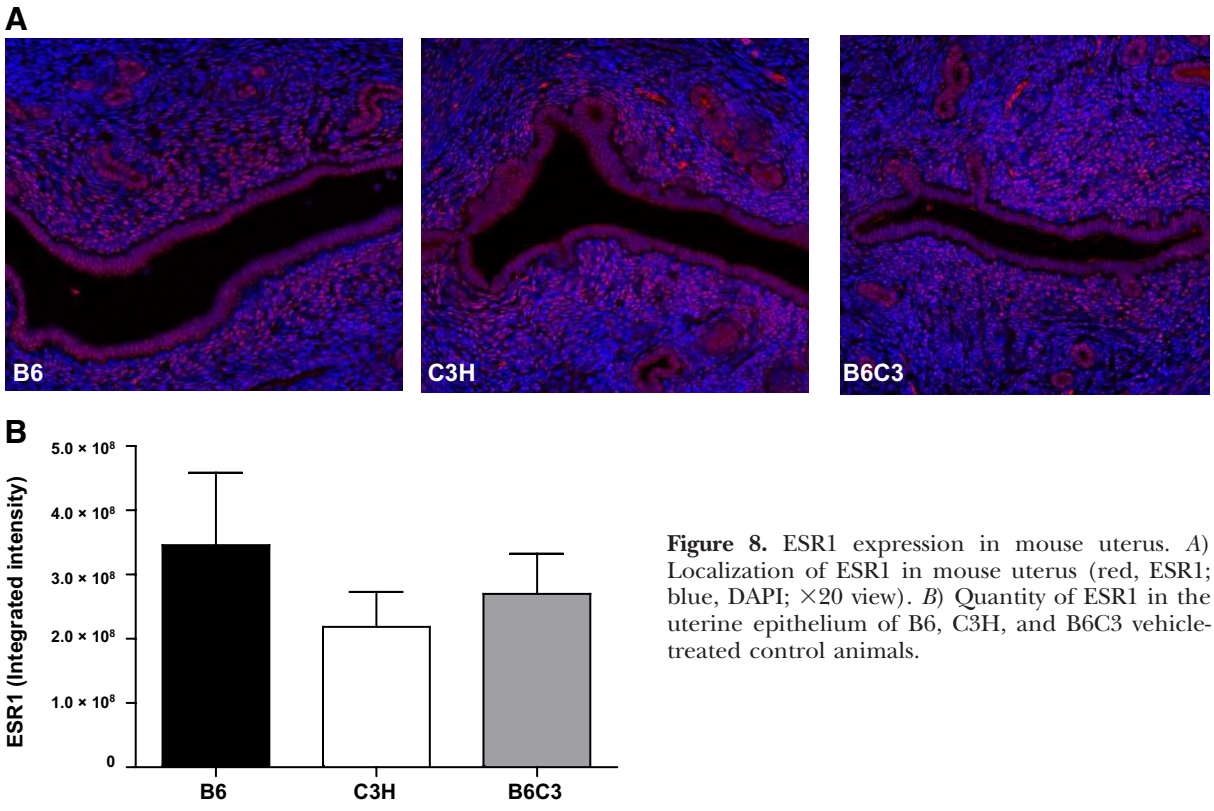

Figure 8. ESR1 expression in mouse uterus. *A*) Localization of ESR1 in mouse uterus (red, ESR1; blue, DAPI; ×20 view). *B*) Quantity of ESR1 in the uterine epithelium of B6, C3H, and B6C3 vehicle-treated control animals.

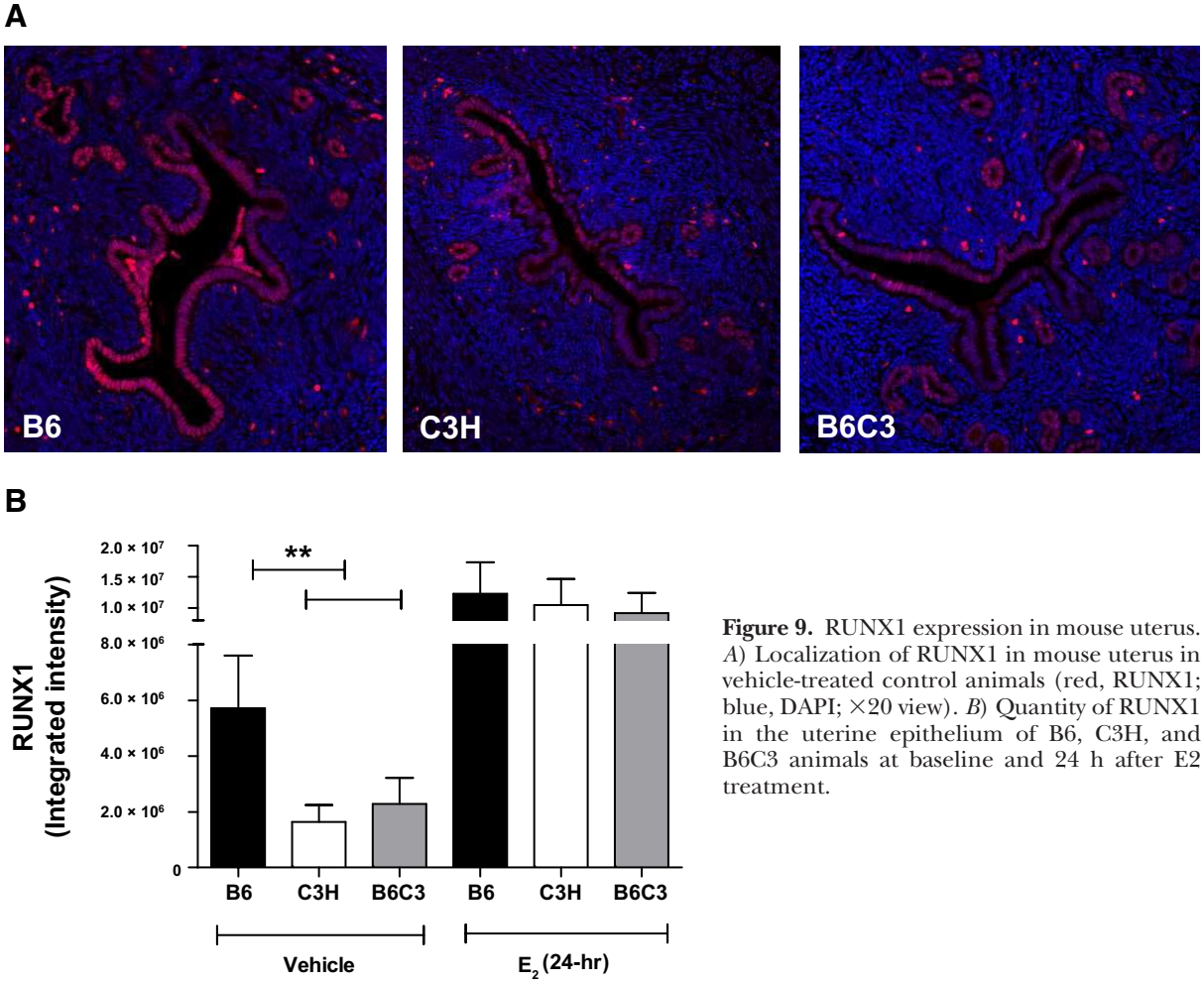

Figure 9. RUNX1 expression in mouse uterus. *A*) Localization of RUNX1 in mouse uterus in vehicle-treated control animals (red, RUNX1; blue, DAPI; ×20 view). *B*) Quantity of RUNX1 in the uterine epithelium of B6, C3H, and B6C3 animals at baseline and 24 h after E2 treatment.

cell death, and cell cycle. All of those cellular functions contribute to the physiological responses of the uterus to E_2, especially cell proliferation, and/or prevention of apoptosis, which is required for the full uterine epithelial response (31).

In addition to the genetic control of E_2-induced changes in uterine weight, the uteri of B6 mice also exhibit a more robust E_2-induced inflammatory responses relative to C3H (12). Consistent with this, acute-phase signaling was significantly enriched at 2 h after E_2 treatment in C3H mice only, and this might have dampened the E_2-induced inflammatory response. The unique acute-phase response in C3H mice may also be responsible for the decreased effect of E_2 on uterine weight in C3H mice relative to B6, since acute-phase proteins are known to be involved in uterine regression and remodeling (32). Indeed, Drasher (7) reported that relative to B6 mice, C3H mice undergo much more extensive uterine regression 6 wk after E_2 treatment. Considering this, and the results of pathway analysis, which indicated an increase in cellular apoptosis in E_2-treated C3H mice relative to B6, we evaluated apoptosis by measuring uterine expression of CC3 and TUNEL 72 h after E_2 treatment. Epithelial cell apoptosis was increased, and expression of the apoptosis inhibitor *Naip1* (*Birc1a*) was decreased, in C3H and B6C3 mice relative to B6. NAIP1 is known to prevent apoptosis by inhibiting CC3 activity in neurons (33); additionally, uteri of *Birc1a*-knockout mice exhibit epithelial apoptosis (34). Thus, it is possible that C3H mice are unable to fully prevent apoptosis immediately following the proliferative response to E_2. As mentioned previously, the prevention of apoptosis is critical for a complete uterine epithelial response (31).

Notably, the results of the microarray experiment reveal that the quantitative differences in the uterotropic response are not simply because of differences in the magnitude of expression of genes within a common shared E_2-regulated transcriptome. Rather, they show that the strain-specific E_2-regulated transcriptomes have both a common shared component and uniquely distinct strain-specific components. Notably, genes that were uniquely regulated in B6 mice were not significantly associated with many cellular functions or pathways, whereas those uniquely regulated in C3H were. This indicates that for B6 mice, the functions associated with the transcriptional response to E_2 were fully represented by common E_2-regulated genes, whereas in C3H mice, unique genes were associated with unique functions and pathways. This has clear functional implications, as illustrated by the association of C3H E_2-regulated genes with cell death, and the observed difference in epithelial cell apoptosis across the strains after E_2 treatment.

Analysis of microarray data of B6C3 mice allowed us to determine the inheritance pattern of E_2-regulated transcripts. To our knowledge, this is the first report describing the inheritance pattern of the E_2-regulated uterine transcriptional program and associated cellular changes. As discussed previously, common E_2-regulated transcripts were identified and may be involved in the proliferative response to E_2; however, the transcriptional response of B6C3 mice to E_2 was in some cases inherited in a mendelian fashion and in other cases exhibited epistatic inheritance. Although the E_2-induced increase in uterine weight of B6C3 mice was C3H-like, the infiltration of immune cells was sometimes intermediate and sometimes B6-like, depending on the type of cell studied (12). Therefore, it is probable that the two phenotypes are inherited independently. Similarly, the transcripts associated with each of these phenotypes are probably inherited independently as well.

Identification of positional candidates underlying QT loci controlling the E_2-regulated uterotropic response

On the basis of the results of SNP analysis we identified many genes containing nonsynonymous SNPs between B6 and C3H mice that reside within the QT loci controlling the uterine response to E_2. These genes were associated with several cellular functions related to the uterotropic response, including tissue development and tissue morphology. Interestingly, many of the polymorphic genes were also differentially expressed at the transcriptional level between B6 and C3H control animals suggesting a role for expression level polymorphisms as candidates in regulating the uterine response to E_2.

To gain insight into the differences that exist between B6 and C3H mice prior to E_2 treatment, we combined microarray analysis on uterine tissue from control animals with data from our genetic mapping experiments (12, 13) and determined that, among the genes differentially expressed at baseline, 84 reside within previously identified QT loci. There were 64 differentially expressed genes that reside within the QT loci for uterine growth, and 20 reside within the QT loci for eosinophil infiltration. Accordingly, we propose that one or more of these genes, since they are differentially expressed between the strains at baseline, are positional candidates controlling the observed differences in the uterine response to E_2 between the two strains. In addition, there were clear differences in the number of leukocytes in the uteri of untreated B6 and C3H animals (12), supporting the concept that at least some of the positional candidates are involved in regulating the infiltration of immune cells both during unstimulated conditions and/or in response to E_2. Moreover, network analysis within IPA revealed that many of the positional candidates are known to interact with ESR1, which was not differentially expressed in control animals (Fig. 8*B*), and this further supports the hypothesis that they are involved in regulating the tissue sensitivity to E_2. Additional physical mapping experiments will be required to positionally clone the polymorphisms underlying the QT loci, and elucidate their mechanism of action in controlling uterine responsiveness to E_2, as well as sensitivity to the actions of endocrine disruptors whose responsiveness is also under genetic control (35, 36).

Identification of *Runx1* as a candidate for epistatic interactions in E_2-regulated responses

Notably, *Runx1* emerged as a candidate for an epistatic modulator of E_2-regulated responsiveness based on its known interaction with ESR1 (22) and the link of *Runx1* to many of the cellular functions that were different between B6 and C3H at baseline. The Runt-related family of transcription factors includes at least 3 transcriptional regulators known to be involved in several cellular processes, including cell proliferation and differentiation (37). A role for *Runx1* has also been suggested in the development of endometrial cancer (38, 39). As mentioned previously, we found that *Runx1* resides within a previously identified QT loci controlling the uterine response to E_2 (12, 13), and there are nearly 300 SNPs that distinguish the B6 *Runx1* allele from that of C3H (http://www.informatics.jax.org/). In addition, *Runx1* mRNA was increased 2 h after E_2 treatment (Supplemental Fig. S2), and uterine expression of RUNX1 was greater in B6 mice compared to C3H mice (Fig. 9*B*). Moreover, RUNX1 has been identified as a potentiator of E_2-induced nonclassical ESR1 signaling [independent of estrogen-response elements (EREs) by acting as a tethering factor; ref. 22]. Although non-ERE signaling comprises only a small percentage of the cellular response to E_2 (21), it has clear biological significance (40), and a subset of E_2-responsive genes is controlled through RUNX1-ESR1 interactions (22). In addition, a preliminary analysis revealed that at least 120 transcripts that were differentially regulated by E_2 in B6 *vs.* C3H mice contain Runx1 motifs (data not shown). To validate the differential expression of these genes, two additional microarray studies were performed using different cohorts of mice and microarray platforms (Affymetrix and Illumina). Of the 120 transcripts, probe sets for 89 were present on all three platforms; of these, expression of 56 probe sets was found to be consistently differentially regulated by E_2 in B6 *vs.* C3H mice across the 3 independent experiments (data for the current microarray experiment is shown in Supplemental Table S1). Consequently, we propose that *Runx1* is a positional candidate for an epistatic interactor contributing to genetic variations in uterine responsiveness to E_2.

Because uterine expression of RUNX1 is greater in B6 mice than C3H, and RUNX1 is an enhancer of E_2-induced cellular responses (22), it is possible that B6 mice are simply poised for a greater overall magnitude of uterine responsiveness to E_2. Restricting ESR1 signaling to the tethered pathway by introducing mutations in the DNA biding domain prevents any growth response of the uterus to E_2 (21), indicating uterine growth requires ESR1 DNA binding function. Nonetheless, non-ERE signaling is thought to comprise nearly 40% of the transcriptional response of the uterus to E_2 at 2 h after treatment and nearly 25% of the response at 24 h after treatment (21). Therefore, it is probable that differences in baseline expression of RUNX1 could

also be associated with strain-specific transcriptional responses to E_2 at both time points, and that RUNX1-mediated tethering contributes to the degree of growth response mediated by ER-ERE-dependent transcripts.

The results of this experiment have shown clear genetic control of both the transcriptional and cellular response of the mouse uterus to E_2. Although we investigated only two genetic backgrounds, previous reports have indicated clear genetic regulation in the response of uterus (7, 8), vagina (8, 9), mammary gland (8), and bone (27, 28) to E_2 across several strains of mice. Therefore, genetics clearly plays a role in phenotypic variation observed in response to natural, synthetic, and environmental estrogens (36, 41, 42). In addition, our findings lay the groundwork for important and relevant experiments that could provide insight into mechanisms underlying genetic variation in other highly relevant E_2-regulated processes in humans, including bone loss in postmenopausal women (43, 44), premature ovarian failure (45), fertility (41, 46), and libido (41), success rate of fertility treatments (42, 47), and sensitivity to environmental endocrine disrupters (36). Future work will be aimed at positionally cloning the genes underlying the QT loci, controlling uterine responsiveness to E_2 and determining their functional role in modulating tissue sensitivity to E_2 across various physiological states and genetic backgrounds. Such analysis is central to understanding inheritance patterns of disease susceptibility and providing insight into how individual genetic variation influences responses to treatment of E_2-dependent diseases and sensitivity to hormonal agents and therapeutics. FJ

The authors thank Stephen Grubb (Jackson Laboratory, Bar Harbor, ME, USA) for assistance with the SNP analysis, the U.S. National Institute of Environmental Health Sciences (NIEHS) Microarray Core for microarray analysis of uterine RNA samples, the NIEHS Histology Laboratory for embedding uterine samples, and the NIEHS Comparative Medicine Branch for surgeries. The staff at the Microscopy Imaging Center at the University of Vermont, funded, in part, by the National Center for Research Resources (1S10RR019246), performed staining and imaging of Runx1 and CC3. S.C.H. and K.S.K. were supported by U.S. National Institutes of Health (NIH) Intramural Research Project Z01ES70065. C.T. was supported by NIH Research Projects R01NS36526, R01NS061014, R01NS060901, R01NS069628, and R01AI41747. The authors declare no conflicts of interest.

REFERENCES

1. Prossnitz, E. R., and Maggiolini, M. (2009) Mechanisms of estrogen signaling and gene expression via GPR30. *Mol. Cell. Endocrinol.* **308,** 32–38
2. Dutertre, M., and Smith, C. L. (2000) Molecular mechanisms of selective estrogen receptor modulator (SERM) action. *J. Pharmacol. Exp. Ther.* **295,** 431–437
3. Katzenellenbogen, B. S., Bhakoo, H. S., Ferguson, E. R., Lan, N. C., Tatee, T., Tsai, T. S., and Katzenellenbogen, J. A. (1979) Estrogen and antiestrogen action in reproductive tissues and tumors. *Recent Prog. Horm. Res.* **35,** 259–300
4. Clark, J. H., and Mani, S. K. (1994) Actions of ovarian steroid hormones. In *The Physiology of Reproduction* (Knobil, E., and Neill, J., eds) **Vol. 1,** pp. 1011–1059, Raven Press, New York
5. Perez, M. C., Furth, E. E., Matzumura, P. D., and Lyttle, C. R. (1996) Role of eosinophils in uterine responses to estrogen. *Biol. Reprod.* **54,** 249–254
6. Hewitt, S. C., Deroo, B. J., Hansen, K., Collins, J., Grissom, S., Afshari, C. A., and Korach, K. S. (2003) Estrogen receptor-dependent genomic responses in the uterus mirror the biphasic physiological response to estrogen. *Mol. Endocrinol.* **17,** 2070–2083
7. Drasher, M. L. (1952) Strain differences in the response of the mouse uterus to estrogens. *J. Hered.* **46,** 190–192
8. Silberberg, M., and Silberberg, R. (1951) Susceptibility to estrogen of breast, vagina, and endometrium of various strains of mice. *Proc. Soc. Exp. Biol. Med.* **76,** 161–164
9. Trentin, J. J. (1950) Vaginal sensitivity to estrogen as related to mammary tumor incidence in mice. *Cancer Res.* **10,** 580–583
10. Blair, S. M., Blair, P. B., and Daane, T. A. (1957) Differences in the mammary response to estrone and progesterone in castrate male mice of several strains and hybrids. *Endocrinology* **61,** 643–651
11. Abiola, O., Angel, J. M., Avner, P., Bachmanov, A. A., Belknap, J. K., Bennett, B., Blankenhorn, E. P., Blizard, D. A., Bolivar, V., Brockmann, G. A., Buck, K. J., Bureau, J. F., Casley, W. L., Chesler, E. J., Cheverud, J. M., Churchill, G. A., Cook, M., Crabbe, J. C., Crusio, W. E., Darvasi, A., de Haan, G., Dermant, P., Doerge, R. W., Elliot, R. W., Farber, C. R., Flaherty, L., Flint, J., Gershenfeld, H., Gibson, J. P., Gu, J., Gu, W., Himmelbauer, H., Hitzemann, R., Hsu, H. C., Hunter, K., Iraqi, F. F., Jansen, R. C., Johnson, T. E., Jones, B. C., Kempermann, G., Lammert, F., Lu, L., Manly, K. F., Matthews, D. B., Medrano, J. F., Mehrabian, M., Mittlemann, G., Mock, B. A., Mogil, J. S., Montagutelli, X., Morahan, G., Mountz, J. D., Nagase, H., Nowakowski, R. S., O'Hara, B. F., Osadchuk, A. V., Paigen, B., Palmer, A. A., Peirce, J. L., Pomp, D., Rosemann, M., Rosen, G. D., Schalkwyk, L. C., Seltzer, Z., Settle, S., Shimomura, K., Shou, S., Sikela, J. M., Siracusa, L. D., Spearow, J. L., Teuscher, C., Threadgill, D. W., Toth, L. A., Toye, A. A., Vadasz, C., Van Zant, G., Wakeland, E., Williams, R. W., Zhang, H. G., and Zou, F.; Complex Trait Consortium (2003) The nature and identification of quantitative trait loci: a community's view. *Nat. Rev. Genet.* **4,** 911–916
12. Griffith, J. S., Jensen, S. M., Lunceford, J. K., Kahn, M. W., Zheng, Y., Falase, E. A., Lyttle, C. R., and Teuscher, C. (1997) Evidence for the genetic control of estradiol-regulated responses. Implications for variation in normal and pathological hormone-dependent phenotypes. *Am. J. Pathol.* **150,** 2223–2230
13. Roper, R. J., Griffith, J. S., Lyttle, C. R., Doerge, R. W., McNabb, A. W., Broadbent, R. E., and Teuscher, C. (1999) Interacting quantitative trait loci control phenotypic variation in murine estradiol-regulated responses. *Endocrinology* **140,** 556–561
14. Padilla-Banks, E., Jefferson, W. N., and Newbold, R. R. (2001) The immature mouse is a suitable model for detection of estrogenicity in the uterotropic bioassay. *Environ. Health Perspect.* **109,** 821–826
15. Himmelhoch, S. R., Evans, W. H., Mage, M. G., and Peterson, E. A. (1969) Purification of myeloperoxidases from the bone marrow of the guinea pig. *Biochemistry* **8,** 914–921
16. Reel, J. R., Lamb, I. J., and Neal, B. H. (1996) Survey and assessment of mammalian estrogen biological assays for hazard characterization. *Fund. Appl. Toxicol.* **34,** 288–305
17. Benjamini, Y., Drai, D., Elmer, G., Kafkafi, N., and Golani, I. (2001) Controlling the false discovery rate in behavior genetics research. *Behav. Brain Res.* **125,** 279–284
18. Hewitt, S. C., and Korach, K. S. (2011) Estrogenic activity of bisphenol A and 2,2-bis(p-hydroxyphenyl)-1,1,1-trichloroethane (HPTE) demonstrated in mouse uterine gene profiles. *Environ. Health Perspect.* **119,** 63–70
19. Tanksley, S. D. (1993) Mapping polygenes. *Ann. Rev. Genet.* **27,** 205–233
20. Mather, K. (1943) Polygenic inheritance and natural selection. *Biol. Rev.* **18,** 32–64
21. Hewitt, S. C., O'Brien, J. E., Jameson, J. L., Kissling, G. E., and Korach, K. S. (2009) Selective disruption of ERα DNA-binding activity alters uterine responsiveness to estradiol. *Mol. Endocrinol.* **23,** 2111–2116
22. Stender, J. D., Kim, K., Charn, T. H., Komm, B., Chang, K. C., Kraus, W. L., Benner, C., Glass, C. K., and Katzenellenbogen, B. S. (2010) Genome-wide analysis of estrogen receptor alpha

DNA binding and tethering mechanisms identifies Runx1 as a novel tethering factor in receptor-mediated transcriptional activation. *Mol. Cell. Biol.* **30,** 3943–3955
23. Hewitt, S. C., and Korach, K. S. (2003) Oestrogen receptor knockout mice: roles for oestrogen receptors alpha and beta in reproductive tissues. *Reproduction* **125,** 143–149
24. Richard, C., Gao, J., Brown, N., and Reese, J. (2003) Aquaporin water channel genes are differentially expressed and regulated by ovarian steroids during the periimplantation period in the mouse. *Endocrinology* **144,** 1533–1541
25. Nagai, J., Yamada, J., Yoshida, M., Chikamune, T., and Naito, M. (1957) Variation of the mammary glands response of inbred female mice treated with estrogen. *Endocrinol. Jpn.* **4,** 12–16
26. Claringbold, P. J., and Biggers, J. D. (1955) The response of inbred mice to oestrogens. *J. Endocrinol.* **12,** 9–14
27. Li, C. Y., Schaffler, M. B., Wolde-Semait, H. T., Hernandez, C. J., and Jepsen, K. J. (2005) Genetic background influences cortical bone response to ovariectomy. *J. Bone. Miner. Res.* **20,** 2150–2158
28. Bouxsein, M. L., Myers, K. S., Shultz, K. L., Donahue, L. R., Rosen, C. J., and Beamer, W. G. (2005) Ovariectomy-induced bone loss varies among inbred strains of mice. *J. Bone Miner. Res.* **20,** 1085–1092
29. Figtree, G. A., Noonan, J. E., Bhindi, R., and Collins, P. (2009) Estrogen receptor polymorphisms: significance to human physiology, disease and therapy. *Recent Patents DNA Gene Seq.* **3,** 164–171
30. Andrew, T., and Macgregor, A. J. (2004) Genes and osteoporosis. *Curr. Osteopor. Rep.* **2,** 79–89
31. Winuthayanon, W., Hewitt, S. C., Orvis, G. D., Behringer, R. R., and Korach, K. S. (2010) Uterine epithelial estrogen receptor alpha is dispensable for proliferation but essential for complete biological and biochemical responses. *Proc. Natl. Acad. Sci. U. S. A.* **107,** 19272–19277
32. Nilsen-Hamilton, M., Liu, Q., Ryon, J., Bendickson, L., Lepont, P., and Chang, Q. (2003) Tissue involution and the acute phase response. *Ann. N. Y. Acad. Sci.* **995,** 94–108
33. Maier, J. K., Lahoua, Z., Gendron, N. H., Fetni, R., Johnston, A., Davoodi, J., Rasper, D., Roy, S., Slack, R. S., Nicholson, D. W., and MacKenzie, A. E. (2002) The neuronal apoptosis inhibitory protein is a direct inhibitor of caspases 3 and 7. *J. Neurosci.* **22,** 2035–2043
34. Yin, Y., Huang, W. W., Lin, C., Chen, H., MacKenzie, A., and Ma, L. (2008) Estrogen suppresses uterine epithelial apoptosis by inducing birc1 expression. *Mol. Endocrinol.* **22,** 113–125
35. Nakai, M., Uchida, K., and Teuscher, C. (1999) The development of male reproductive organ abnormalities after neonatal exposure to tamoxifen is genetically determined. *J. Androl.* **20,** 626–634
36. Spearow, J. L., Doemeny, P., Sera, R., Leffler, R., and Barkley, M. (1999) Genetic variation in susceptibility to endocrine disruption by estrogen in mice. *Science* **285,** 1259–1261
37. Ito, Y. (2008) RUNX genes in development and cancer: regulation of viral gene expression and the discovery of RUNX family genes. *Adv. Cancer Res.* **99,** 33–76
38. Doll, A., Gonzalez, M., Abal, M., Llaurado, M., Rigau, M., Colas, E., Monge, M., Xercavins, J., Capella, G., Diaz, B., Gil-Moreno, A., Alameda, F., and Reventos, J. (2009) An orthotopic endometrial cancer mouse model demonstrates a role for RUNX1 in distant metastasis. *Int. J. Cancer* **125,** 257–263
39. Planaguma, J., Abal, M., Gil-Moreno, A., Diaz-Fuertes, M., Monge, M., Garcia, A., Baro, T., Xercavins, J., Reventos, J., and Alameda, F. (2005) Up-regulation of ERM/ETV5 correlates with the degree of myometrial infiltration in endometrioid endometrial carcinoma. *J. Pathol.* **207,** 422–429
40. Meyer, M. R., Haas, E., Prossnitz, E. R., and Barton, M. (2009) Non-genomic regulation of vascular cell function and growth by estrogen. *Mol. Cell. Endocrinol.* **308,** 9–16
41. Simpson, E. R., and Jones, M. E. (2006) Of mice and men: the many guises of estrogens. *Ernst Schering Found. Symp. Proc.* 45–67
42. Altmae, S., Hovatta, O., Stavreus-Evers, A., and Salumets, A. (2011) Genetic predictors of controlled ovarian hyperstimulation: where do we stand today? *Hum. Reprod. Update* **17,** 813–828
43. Riggs, B. L., Khosla, S., and Melton, L. J., 3rd (1998) A unitary model for involutional osteoporosis: estrogen deficiency causes both type I and type II osteoporosis in postmenopausal women and contributes to bone loss in aging men. *J. Bone Miner. Res.* **13,** 763–773
44. Richards, J. B., Zheng, H. F., and Spector, T. D. (2012) Genetics of osteoporosis from genome-wide association studies: advances and challenges. *Nat. Rev. Genet.* **13,** 576–588
45. Beck-Peccoz, P., and Persani, L. (2006) Premature ovarian failure. *Orphanet J. Rare Dis.* **1,** 9
46. Krausz, C., and Giachini, C. (2007) Genetic risk factors in male infertility. *Arch. Androl.* **53,** 125–133
47. Loutradis, D., Theofanakis, C., Anagnostou, E., Mavrogianni, D., and Partsinevelos, G. A. (2012) Genetic profile of SNP(s) and ovulation induction. *Curr. Pharm. Biotechnol.* **13,** 417–425

Received for publication June 19, 2012.
Accepted for publication January 14, 2013.